Journal of Chromatography, 396 (1987) 149–155
Elsevier Science Publishers B.V., Amsterdam — Printed in The Netherlands

CHROM. 19 507

INDIRECT PHOTOMETRIC DETECTION OF HYDROCARBONS IN MICRO HIGH-PERFORMANCE LIQUID CHROMATOGRAPHY

TOYOHIDE TAKEUCHI* and DAIDO ISHII
Department of Applied Chemistry, Faculty of Engineering, Nagoya University, Chikusa-ku, Nagoya 464 (Japan)
(Received February 16th, 1987)

SUMMARY

Indirect photometric detection of hydrocarbons was investigated in micro high-performance liquid chromatography. An aromatic hydrocarbon was added in the mobile phase to maintain a background. Hydrocarbons were sensitively detected owing to their perturbation of the partitioning characteristics of the visualization agent. Subnanogram detection limits were achieved.

INTRODUCTION

Indirect photometric or fluorometric detection of non-electrolytes in high-performance liquid chromatography (HPLC) has been investigated[1–12]. The principle of indirect detection of non-electrolytes involves ion-pair formation between the analytes and the visualization agent[1–3], perturbation of the partitioning characteristics of the latter due to the analytes[6–8,10–12] and variation of its solubility in the mobile phase due to the analytes[9].

The minimum detectable concentration of the analyte in the detector is given by[12]

$$C_s > \frac{C_m}{D_R(R + C_m V_s - RC_m V_m) + C_m(RV_m - V_s)} \quad (1)$$

where C_s is the concentration of the analyte in the detector, C_m is the concentration of the visualization agent, D_R is the dynamic reserve (defined as the ratio of the background to its noise level), R is the displacement ratio (defined as the number of visualization species transferred by one analyte species), V_s is the volume of 1 mol of the analyte and V_m is the volume of 1 mol of the visualization agent. Since it has been observed that the displacment ratio is much smaller than 1 in indirect detection of non-electrolytes, and that the dynamic reserve is much larger than 1[11], the minimum detectable concentration can be represented by:

$$C_s > \frac{1}{D_R(R/C_m + V_s)} \quad (2)$$

0021-9673/87/$03.50

Eqn. 2 indicates that the limit of detection is inversely proportional to the dynamic reserve. In previous work[12] the limit of detection for alcohols was subnanogram. The detectability of the analytes of interest could be improved by appropriate selection of the visualization agent because the analytes eluting close to the system peak gave larger signals.

This paper describes the indirect photometric detection of hydrocarbons. Detection of hydrocarbons in kerosine and benzine will be demonstrated.

EXPERIMENTAL

The chromatographic system was the same as in the previous work[12], comprising a syringe-type pump, a micro valve injector, a fused-silica micropacked column, a water-bath and an UV detector. A Micro Feeder (Azumadenki Kogyo, Tokyo, Japan) equipped with a 0.5-ml gas-tight syringe was employed as a pump. A variable-wavelength UV spectrophotometer UVIDEC-100V (Jasco, Tokyo, Japan) was employed as a detector. The sample (18 nl) was injected with an ML-422 micro valve injector (Jasco). The separation column was immersed in the water-bath in order to avoid variations in the ambient temperature, otherwise very noisy baselines were observed. Hydrocarbons, polynuclear aromatic hydrocarbons, acetonitrile and HPLC-grade distilled water were supplied by Wako (Osaka, Japan) or Tokyo Chemical Industry (Tokyo, Japan), and they were used without any purification. Chemically bonded silica packings, ODS SC-01 (5 μm; Jasco) and Develosil ODS-3K (3 μm; Nomura Chemical, Seto, Japan), were employed and the separation columns were prepared in the laboratory by the method previously reported[13].

RESULTS AND DISCUSSION

The principle of indirect detection of non-electrolytes is quite different from

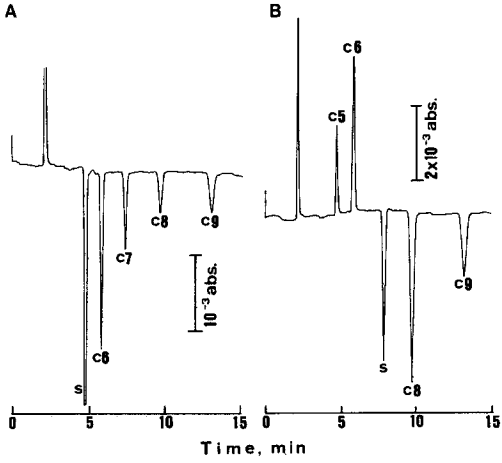

Fig. 1. Indirect photometric detection of hydrocarbons using anthracene or chrysene as the visualization agent. Column: ODS SC-01, 150 mm × 0.34 mm I.D. Mobile phase: acetonitrile–water (90:10) including $8 \cdot 10^{-5}$ *M* anthracene (A) or chrysene (B). Flow-rate: 4.2 μl/min. Sample: 1% (v/v) each; the carbon numbers of the *n*-alkanes are shown. Wavelengths of UV detection: 250 (A) and 269 nm (B).

TABLE I

DISPLACEMENT RATIO AND SIGNAL INTENSITIES

Operating conditions as inFig. 1.

Analyte	*Displacement ratio*		*Relative signal intensity*	
	Fig. 1A	*Fig. 1B*	*Fig. 1A*	*Fig. 1B*
Pentane	–	$9.1 \cdot 10^{-4}$	–	26
Hexane	$1.1 \cdot 10^{-3}$	$2.2 \cdot 10^{-3}$	34	56
Heptane	$6.7 \cdot 10^{-4}$	–	19	–
Octane	$4.6 \cdot 10^{-4}$	$4.9 \cdot 10^{-3}$	12	100
Nonane	$3.9 \cdot 10^{-4}$	$2.7 \cdot 10^{-3}$	9	52

that of ionic species. When the analyte varies the partitioning characteristics of the visualization species which have been equilibrated between the mobile and the stationary phase, the analytes can be indirectly detected by variation of the background.

Fig. 1 demonstrates indirect detection of hydrocarbons (pentane to nonane) using anthracene or chrysene as the visualization agent. The retention time of the system peak (S) coincides with that of anthracene in Fig. 1A and chrysene in Fig. 1B, respectively. The analytes eluted before the system peak give positive peaks, while the analytes eluted after the system peak give negative peaks. This indicates that all the analytes in Fig. 1 transfer the visualization species from the stationary phase to the mobile phase, as discussed in the literature[14]. The analytes eluted close to the system peak give larger signals, which indicates that we can improve the detectability of the analytes of interest by appropriate selection of the visualization species. The detectability of octane is improved by a factor of 8.1 in Fig. 1B in comparison with that in Fig. 1A. Under the conditions in Fig. 1B, resolution of heptane and the system peak was not achieved. When heptane was injected under the conditions in Fig. 1B a large differential peak was observed.

Displacement ratios were calculated from the chromatographic data in Fig. 1, *viz.*, peak heights, peak volumes and the background levels. The results are shown

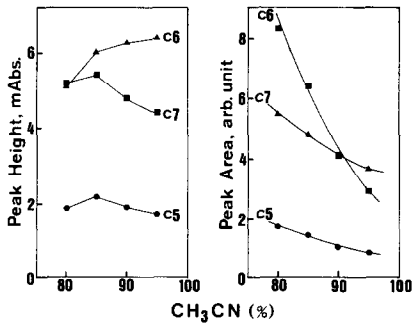

Fig. 2. Effects of the mobile phase composition on signal intensities. Column: Develosil ODS-3K, 100 mm × 0.26 mm I.D. Mobile phase: acetonitrile–water including $8 \cdot 10^{-5}$ *M* chrysene. Flow-rate: 2.1 μl/min. Sample: 0.5% (v/v) each. Wavelength of UV detection: 269 nm.

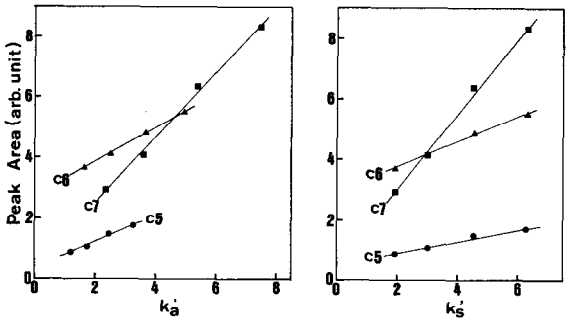

Fig. 3. Plots of peak areas *versus* the capacity factor of the analyte, k'_a, or of the system peak, k'_s. Operating conditions as in Fig. 2.

in Table I together with the relative signal intensities (peak areas). It is seen that the displacement ratio is much smaller than 1.

The effects of the mobile phase composition on the signal intensities are shown in Fig. 2, in which chrysene is used as the visualization agent. The peak areas decrease with increasing content of acetonitrile in the mobile phase, while plots of the peak height *versus* the mobile phase composition are convex curves and the composition corresponding to the maximum peak height depends on the analyte.

The peak areas are plotted *versus* the capacity of the analyte, k'_a, and of the system peak (chrysene, k'_s) in Fig. 3. It is seen that the peak areas increase with increasing k'_a and k'_s. Corrected capacity factors are given in this paper, *viz.*, the instrumental dead volume (0.79 μl) was subtracted from the observed retention volumes and the void volume.

The results obtained led us to plot the peak area *versus* $k'_s/(\alpha - 1)$, where α is the separation factor which is given by k'_s/k'_a when $k'_s > k'_a$ and by k'_a/k'_s when $k'_s < k'_a$. Fig. 4 illustrates this relationship using chrysene as the visualization agent. A good correlation is observed regardless of the analytes and the mobile phase composition, although we have not considered the difference in the degree of perturbation

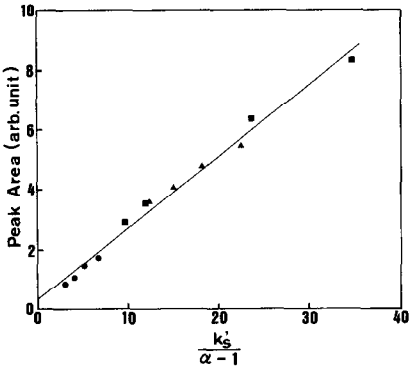

Fig. 4. Relationship between the signal intensity and $k'_s/(\alpha - 1)$. ●, Pentane; ▲, hexane; ■, heptane Operating conditions as in Fig. 2.

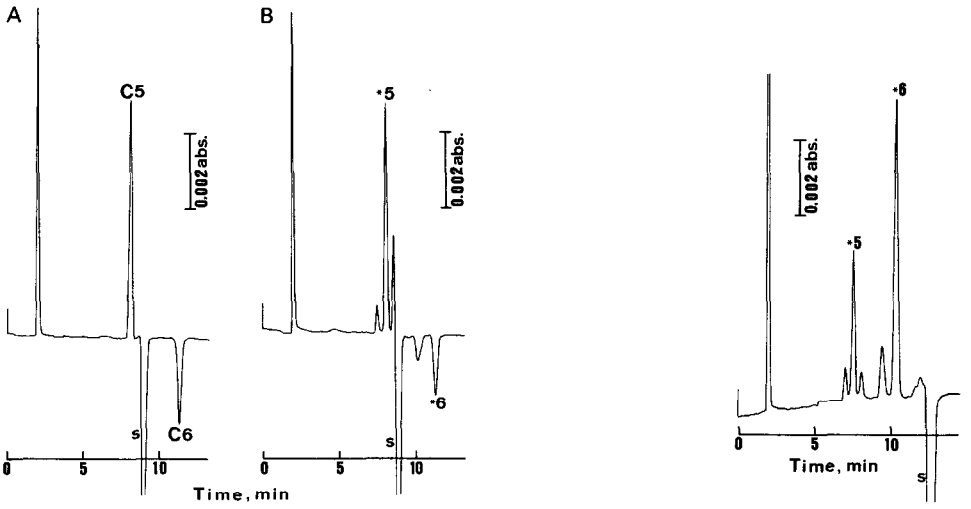

Fig. 5. Indirect photometric detection of an artificial mixture of pentane (C_5) and hexane (C_6) and components in light petroleum using anthracene as the visualization agent. Column: ODS SC-01, 150 mm × 0.34 mm I.D. Mobile phase: acetonitrile–water (75:25) including $6 \cdot 10^{-5}$ *M* anthracene. Flow-rate: 4.2 µl/min. Sample: 1% (v/v) each (A); and 2% (v/v) light petroleum (B). Wavelength of UV detection: 250 nm.

Fig. 6. Indirect photometric detection of components in light petroleum using chrysene as the visualization agent. Column: Develosil ODS-3K, 100 mm × 0.26 mm I.D. Mobile phase: acetonitrile–water (80:20) including $8 \cdot 10^{-5}$ *M* chrysene. Flow-rate: 2.1 µl/min. Sample: 2% (v/v) light petroleum. Wavelength of UV detection: 269 nm.

of the partitioning characteristics due to the analytes. The stationary phase, the visualization agent and the background level can also affect the signal intensity. The background level may be compensated by plotting the signal intensity divided by the background signal. If we assume that the peak area is proportional to $k_s'/(\alpha - 1)$, the peak height (P.H.) can be represented by

$$\text{P.H.} = \frac{Ak_s'CB_GKN^{\frac{1}{2}}}{(\alpha - 1)(1 + k_a')V_0} \tag{3}$$

where A is a constant, B_G is the background level, C is the concentration of the

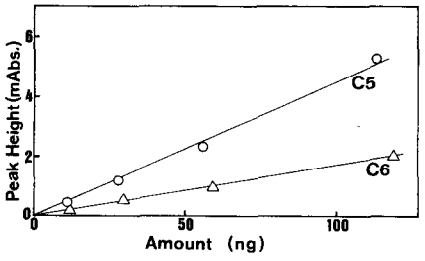

Fig. 7. Relationships between the peak height and the amounts of the analytes injected. Operating conditions as in Fig. 5A.

analyte injected, K is a coefficient which accounts for the degree of perturbation of the partitioning characteristics due to the analyte, N is the theoretical plate number and V_0 is the void volume of the separation column; B_G, N and V_0 are constant under the same operating conditions. Theoretical treatments concerning the chromatographic process will be necessary to predict the signal intensity.

Fig. 5 demonstrates the indirect photometric detection of an artificial mixture of hydrocarbons and components in light petroleum (b.p. 30–70°C) using anthracene as the visualization agent. Peaks noted by "*5" and "*6" in Fig. 5B were eluted at the same retention times as those of pentane and hexane, respectively.

Fig. 6 demonstrates the indirect detection of components in light petroleum under different conditions. Chrysene is used as the visualization agent.

Fig. 7 illustrates the relationships between the peak height and the amounts of the analytes injected. Linear relationships were observed up to 120 ng. The limit of detection depended on the operating conditions, *e.g.*, relative retention time of the analyte *versus* the visualization species and the dynamic reserve. A dynamic reserve

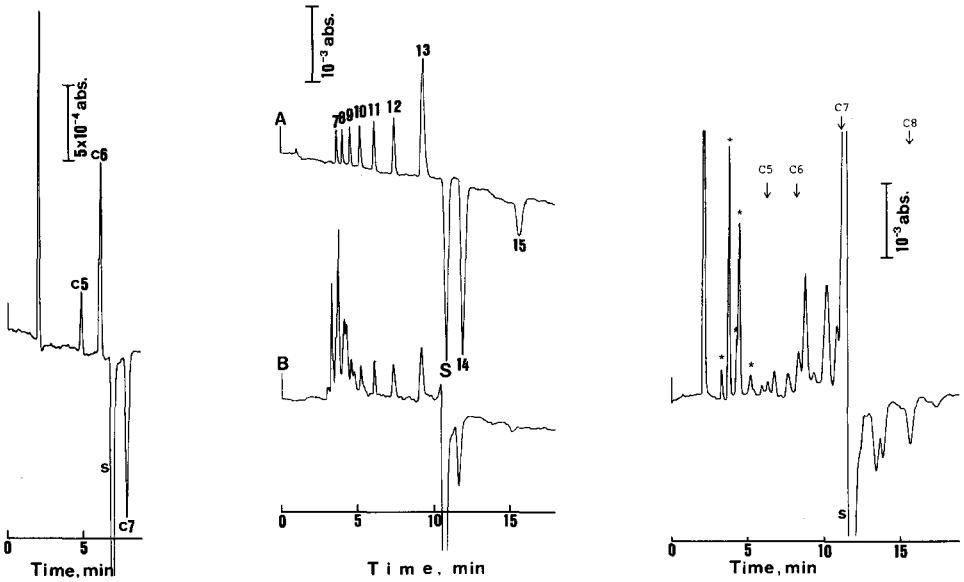

Fig. 8. Indirect photometric detection of small amounts of hydrocarbons. Column: Develosil ODS-3K, 100 mm × 0.26 mm I.D. Mobile phase: acetonitrile–water (90:10) including $8 \cdot 10^{-5}$ M chrysene. Flow-rate: 2.1 μl/min. Sample: 11 ng of pentane (C_5), 12 ng of hexane (C_6) and 12 ng of heptane (C_7). Wavelength of UV detection: 269 nm.

Fig. 9. Indirect photometric detection of an artificial mixture of hydrocarbons and components in kerosine. Column: ODS SC-01, 150 mm × 0.34 mm I.D. Mobile phase: methanol including $1.2 \cdot 10^{-4}$ M benzo[*a*]pyrene. Flow-rate: 4.2 μl/min. Sample: 0.5% (v/v) each; the numbers correspond to the carbon numbers of straight-chain hydrocarbons (A); and 6.7% (v/v) kerosine (B). Wavelength of UV detection: 300 nm.

Fig. 10. Indirect photometric detection of components in benzine. Column: ODS SC-01, 150 mm × 0.34 mm I.D. Mobile phase: acetonitrile–water (82:18) including $8 \cdot 10^{-5}$ M chrysene. Flow-rate: 4.2 μl/min. Sample: 3% (v/v) benzine. Wavelength of UV detection: 269 nm.

of *ca.* 20000 was achieved with the best conditions in this system, and the limit of detection was subnanogram.

Fig. 8 demonstrates the indirect photometric detection of pentane, hexane and heptane; *ca.* 10 ng of each analyte were injected. The detection limit at S/N = 2 was 0.8 ng for pentane, 0.3 ng for hexane and heptane.

Fig. 9 demonstrates the indirect detection of an artificial mixture of hydrocarbons (heptane to pentadecane) and components in kerosine using benzo[*a*]pyrene as the visualization agent. The volume of kerosine injected corresponds to 1.2 nl (18 nl of 6.7%). Several peaks were eluted at the same retention times as those of straight-chain hydrocarbons. If we assume that these peaks were due to the straight-chain hydrocarbons, we could determine their concentrations.

Fig. 10 demonstrates the separation of components in petroleum benzine (b.p. 40–150°C) (fuel for a body warmer). Several peaks denoted by "*" originally absorbed UV light and the other peaks were detected indirectly. The retention times of the *n*-alkanes are shown in the chromatogram. Coupling of micro HPLC and capillary gas chromatography will help in the analysis of complex mixtures.

CONCLUSION

Hydrocarbons were indirectly detected by using appropriate polynuclear aromatic hydrocarbons as the visualization agent. The detectability of the analytes of interest could be improved by appropriate selection of the visualization species. Subnanogram detection limits were achieved.

REFERENCES

1 T. Gnanasambandan and H. Freiser, *Anal. Chem.*, 53 (1981) 909.
2 T. Gnanasambandan and H. Freiser, *Anal. Chem.*, 54 (1982) 1282.
3 T. Gnanasambandan and H. Freiser, *Anal. Chem.*, 54 1982) 2379.
4 S. Y. Su, A. Jurgensen, D. Bolton and J. D. Winefordner, *Anal. Lett.*, 14 (1981) 1.
5 L. Hackzell and G. Schill, *Chromatographia*, 15 (1982) 437.
6 J. E. Parkin, *J. Chromatogr.*, 287 (1984) 457.
7 G. Vigh and A. Leitold, *J. Chromatogr.*, 312 (1984) 345.
8 J. E. Parkin and H. T. Lau, *J. Chromatogr.*, 314 (1984) 488.
9 S. Banerjee, *Anal. Chem.*, 57 (1985) 2590.
10 T. Takeuchi and E. S. Yeung, *J. Chromatogr.*, 366 (1986) 145.
11 P. K. Gupta and J. G. Nikelly, *J. High Resolut. Chromatogr. Chromatogr. Commun.*, 9 (1986) 572.
12 T. Takeuchi and D. Ishii, *J. Chromatogr.*, 393 (1987) 419.
13 T. Takeuchi and D. Ishii, *J. Chromatogr.*, 213 (1981) 25.
14 J. J. Stranahan and S. N. Deming, *Anal. Chem.*, 54 (1982) 1540.